THE JOURNAL OF BIOLOGICAL CHEMISTRY VOL. 286, NO. 4, pp. 2750–2761, January 28, 2011

Streptolysin S Contributes to Group A Streptococcal Translocation across an Epithelial Barrier*[S]

Received for publication, August 9, 2010, and in revised form, October 22, 2010 Published, JBC Papers in Press, November 17, 2010, DOI 10.1074/jbc.M110.171504

Tomoko Sumitomo[‡], Masanobu Nakata[‡], Miharu Higashino[‡], Yingji Jin[§], Yutaka Terao[‡], Yukako Fujinaga[§], and Shigetada Kawabata[‡1]

From the [‡]Department of Oral and Molecular Microbiology, Osaka University Graduate School of Dentistry, 1-8 Yamadaoka, Suita, Osaka 565-0871, Japan and the [§]Laboratory for Infection Cell Biology, International Research Center for Infectious Diseases, Research Institute for Microbial Diseases, Osaka University, 3-1 Yamadaoka, Suita, Osaka 565-0871, Japan

Group A *Streptococcus pyogenes* (GAS) is a human pathogen that causes local suppurative infections and severe invasive diseases. Systemic dissemination of GAS is initiated by bacterial penetration of the epithelial barrier of the pharynx or damaged skin. To gain insight into the mechanism by which GAS penetrates the epithelial barrier, we sought to identify both bacterial and host factors involved in the process. Screening of a transposon mutant library of a clinical GAS isolate recovered from an invasive episode allowed identification of streptolysin S (SLS) as a novel factor that facilitates the translocation of GAS. Of note, the wild type strain efficiently translocated across the epithelial monolayer, accompanied by a decrease in transepithelial electrical resistance and cleavage of transmembrane junctional proteins, including occludin and E-cadherin. Loss of integrity of intercellular junctions was inhibited after infection with a deletion mutant of the *sagA* gene encoding SLS, as compared with those infected with the wild type strain. Interestingly, following GAS infection, calpain was recruited to the plasma membrane along with E-cadherin. Moreover, bacterial translocation and destabilization of the junctions were partially inhibited by a pharmacological calpain inhibitor or genetic interference with calpain. Our data indicate a potential function of SLS that facilitates GAS invasion into deeper tissues via degradation of epithelial intercellular junctions in concert with the host cysteine protease calpain.

An epithelial barrier is the first line of host defense against most human pathogens. Cell-cell and cell-matrix junctional complexes are important for the development of polarized epithelium and an intact barrier. Individual epithelial cells are joined to each other by specialized complexes, including tight junctions (TJs)[2] and adherence junctions (1), and their disruption may allow pathogens to disseminate infection. Therefore, a number of pathogens have evolved unique strategies to target intercellular junctions and their components (2–4).

Streptococcus pyogenes (group A streptococci; GAS) is a β-hemolytic organism responsible for a wide variety of human diseases that most commonly occur as self-limiting purulent infections of the pharynx and skin (5). GAS also causes non-suppurative sequelae, such as rheumatic fever and glomerulonephritis, which are serious problems in developing countries (6). Although the occurrence of GAS invasive infections, including necrotizing fasciitis and streptococcal toxic shock syndrome, is rare, mortality rates remain high even with progressive medical therapy (7). Invasive disease may occur by either progression of an antecedent superficial infection or direct inoculation from a penetrating injury.

In the early stages of infection, GAS must gain contact with superficial epithelial cells of the pharynx or skin. To establish colonization at those anatomical sites, firm bacterial adherence to epithelial cells and escape from the immune system are indispensable. Both the pharynx and skin are guarded by the epithelial barrier apposed tightly by TJs and adherence junctions. Thus, as a prerequisite for causing severe invasive disease, GAS must invade the underlying sterile tissues *per se*, which is accomplished by translocation across the epithelial barrier together with evasion of host defense mechanisms.

Many researchers have postulated that GAS possesses strategies to overcome the epithelial barrier via the paracellular route or "intracellular route" (8–10). Over the past several decades, the molecular mechanisms underlying the adherence and internalization of GAS to epithelial cells as well as their intricate interactions have been extensively studied (8–12). Although it was considered that most internalized GAS organisms are eliminated by intracellular killing, massive internalization or adherence of GAS preferentially induces programmed cell death of epithelial cells (13–15). These processes may lead to exposure of underlying tissues or cause damage to epithelium, providing GAS with a route to deeper tissues (intracellular route). However, not all GAS strains isolated from patients with invasive diseases possess the ability

* This work was supported by Grant-in-Aid for Scientific Research for Young Scientists (B) 20791336 from the Ministry of Education, Culture, Sports, Science, and Technology (MEXT) (to T. S.); Grant-in-Aid for Scientific Research on Priority Areas 18073011 from MEXT (to S. K.); Grant-in-Aid for Scientific Research (B) 20390465 from the Japan Society for the Promotion of Science (JSPS) (to S. K.); Grant-in-Aid for Scientific Research for Young Scientists (A) 2189048 from MEXT (to Y. T.); and Grant-in-Aid for Scientific Research for Young Scientists (B) 19791343 from MEXT (to M. N.).

[S] The on-line version of this article (available at http://www.jbc.org) contains supplemental Table S1 and Figs. S1–S3.

[1] To whom correspondence should be addressed: Dept. of Oral and Molecular Microbiology, Osaka University Graduate School of Dentistry, 1-8, Yamadaoka, Suita, Osaka 565-0871, Japan. Tel.: 81-6-6879-2896; Fax: 81-6-6879-2180; E-mail: kawabata@dent.osaka-u.ac.jp.

[2] The abbreviations used are: TJ, tight junction; GAS, group A *S. pyogenes*; SLS, streptolysin S; TER, transepithelial electrical resistance; MOI, multiplicity of infection; LDH, lactate dehydrogenase; EGFP, enhanced green fluorescence protein.

to internalize epithelial cells with a high frequency. Indeed, Cywes and Wessels (16) reported that GAS tissue invasion occurs via a paracellular route. They analyzed a detailed mechanism of the GAS invasion and clarified that interactions of hyaluronic acid, a component of the capsule, with CD44 induce marked cytoskeletal rearrangements, including membrane ruffling and disruption of intercellular junctions (16). Moreover, Pezzicoli *et al.* (17) reported that group B streptococcus also crosses the epithelial barrier by a paracellular route. Therefore, infectious strategies via the paracellular route have been noted in the streptococcal infections.

Because GAS infection has a multifactorial nature and we found a clinical isolate showing a high translocation ability despite low capsule production, we postulated that alternative bacterial factors might be involved in the translocation process. To search for novel factors manipulating this process, we screened a Tn*916* mutant library based on the ability to translocate across a model of the epithelial barrier. Herein, we report that streptolysin S (SLS), a determinant for β-hemolysis, facilitates the translocation of GAS via degradation of intercellular junctions associated with the epithelial barrier in concert with host proteases.

EXPERIMENTAL PROCEDURES

Bacterial Strains and Culture Conditions—GAS clinical isolates, strains NIH35 (serotype 28), SSI-1 (serotype 3), SSI-9 (serotype 1), and 30 (serotype 12), isolated from patients with streptococcal toxic shock syndrome, were kindly provided by Drs. H. Watanabe (National Institute of Infectious Diseases, Japan) and T. Murai. *Escherichia coli* XL10-Gold (Stratagene) and Top10 (Invitrogen) were used as hosts for plasmids pAT18 and pSET4s (18, 19). *Enterococcus faecalis* CG110 served as a Tn*916* donor strain (20). *E. faecalis* and GAS strains were cultured at 37 °C in Todd-Hewitt broth (BD Biosciences) supplemented with 0.2% yeast extract (BD Biosciences) (THY medium). *E. coli* strains were cultured in Luria-Bertani (Sigma) (LB) medium at 37 °C with agitation. For selection and maintenance of the mutants, antibiotics were added to the media at the following concentrations: ampicillin, 100 μg/ml for *E. coli*; erythromycin, 150 μg/ml for *E. coli* and 1 μg/ml for GAS; kanamycin, 300 μg/ml for GAS; spectinomycin, 100 μg/ml for *E. coli* and GAS; streptomycin, 1 mg/ml for GAS; and tetracycline, 10 μg/ml for *E. faecalis* and GAS.

Quantitative Analysis of Capsule Production—The amount of hyaluronic acid on the GAS cell surface was measured using a hyaluronan enzyme-linked immunosorbent assay kit (Echelon Biosciences), according to the manufacturer's instructions. GAS strains were grown to an exponential phase (A_{600} = 0.4) and centrifuged at 7,000 × *g* for 5 min. Pelleted cells were resuspended in phosphate-buffered saline (PBS) and heat-killed at 65 °C for 30 min and then centrifuged at 13,000 × *g* for 5 min. The resultant supernatants were used to determine hyaluronic acid production.

Construction of GAS Mutant Strains—For construction of the *sagA* in-frame deletion mutant, the primers slskoF1 and slskoR1 (supplemental Table S1) were utilized with PCR to amplify the upstream flanking sequence and start codon of the *sagA* gene, with chromosomal DNA of strain NIH35 as a template. The downstream flanking sequence and stop codon of the *sagA* gene were amplified using primers slskoF2 and slskoR2 (supplemental Table S1). The two generated PCR products containing complementary ends were purified using NucleoSpin Extract II (Macherey-Nagel). Subsequently, overlap PCR was performed with mixed PCR products as a template and primers slskoF1 and slskoR2. The overlap PCR product was digested with EcoRI and BamHI and cloned into the temperature-sensitive shuttle vector pSET4s via EcoRI/BamHI sites. The resultant plasmid pSET4s-*sagA*KO was transformed into strain NIH35 by electroporation. Transformants were grown at 30 °C and selected on THY agar plates containing spectinomycin. A single colony was subjected to serial passages in the presence of spectinomycin at 37 °C twice, followed by a serial passage at 30 °C without spectinomycin. Finally, spectinomycin-sensitive colonies were tested for deletion of the *sagA* gene by PCR using primers sagCheckF and sagCheckR (supplemental Table S1). Correct deletion of the *sagA* gene was confirmed by sequence analysis of the chromosomal locus encompassing the recombination sites.

To repair the mutation in the *sagA* deletion mutant, a pSET4s plasmid containing the *sagA* gene and flanking region was transformed into the *sagA* mutant. Introduction of the *sagA* gene into the *sagA*-deleted chromosomal region was achieved as described above.

The *hasA* mutant was constructed by insertional inactivation using pSK147 (12). Correct insertion of a kanamycin-resistant cassette into GAS genomic DNA was confirmed by site-specific PCR, using primers hasCheckF and hasCheckR (supplemental Table S1).

For construction of EGFP-expressing GAS strains, a pAT18-EGFP vector was transformed into the GAS strains by electroporation (13). The transformants were selected on THY agar plates containing erythromycin.

Cells—Caco-2 cells (Riken Cell Bank), a human colon carcinoma epithelial cell line, were maintained in minimum essential medium (Life Technologies) supplemented with 20% fetal bovine serum (SAFC Biosciences), 20 μg/ml gentamicin, 17.75 mM $NaHCO_3$ (Wako), and 15 mM HEPES (Dojindo) at pH 7.4.

To obtain the human keratinocyte cell line HaCaT, we first received permission from Dr. N. Fusenig and purchased it from Dr. R. Steubing. HaCaT cells were maintained in Dulbecco's modified Eagle's medium (Wako) supplemented with 10% fetal bovine serum (SAFC Biosciences) and 20 μg/ml gentamicin.

Translocation and Antibiotic Protection Assays—Caco-2 cells and HaCaT cells were seeded at 4 × 10^5 cells/well onto polycarbonate Millicell culture plate inserts (12-well plates, 3-μm pore size; Millipore) and cultured for 3–5 days at 37 °C under a 5% CO_2 atmosphere with daily medium changes. To determine the Caco-2 monolayer integrity, transepithelial electrical resistance (TER) of the filter-grown monolayers was measured by a Millicell-ERS (Millipore). Caco-2 monolayers exhibiting TER of 450–500 ohms·cm^2 were used for translocation assays. The integrity of the HaCaT monolayers was not detectable by TER measurement (21). Therefore, polarized

monolayers were determined using a fluorescein permeability assay. DMEM containing 0.02% sodium fluorescein was added to the apical surface of filter-grown HaCaT monolayers, and they were incubated for 6 h at 37 °C under a 5% CO_2 atmosphere. After incubation, the amount of sodium fluorescein in the basolateral medium was measured using an absorption spectrometer (A_{490}). A HaCaT monolayer was accepted as polarized if the paracellular flux of fluorescein from apical to basolateral medium was not detectable after incubation. Polarized monolayers were infected with GAS at a multiplicity of infection (MOI) of 10. To remove non-adherent bacteria, the medium in the upper chamber was replaced with fresh medium at 2 h after infection. The ability of the GAS strains to translocate into the monolayers was assessed by quantitative cultures of medium obtained from the lower chambers at various times after infection. For those assays, each medium sample was serially diluted and plated on THY agar plates to determine CFU. For quantification of bacterial adhesion, infected monolayers were washed with PBS and lysed with distilled water. To determine bacterial internalization, extracellular GAS organisms were killed by treatment with penicillin (60 μg/ml) and gentamicin (100 μg/ml) for 1 h, and then intracellular GAS was recovered after lysis of the monolayers. The numbers of adhered or internalized bacteria were assessed as described above. In some experiments, calpain inhibitors, calpeptin (Calbiochem) and ALLN (Calbiochem), and a proteasome inhibitor MG-115 (Sigma) were added to Caco-2 monolayers 1 h before infection.

Immunofluorescence Confocal Microscopy—Caco-2 cells and HaCaT cells were seeded at 2×10^5 cells/well onto coverslides pretreated with poly-L-lysine (13-mm diameter; Matsunami) and cultured for 3 days at 37 °C under a 5% CO_2 atmosphere. The cells were infected with EGFP-expressing GAS strains at an MOI of 10 for various time periods and then fixed with 4% paraformaldehyde in PBS for 20 min at room temperature, followed by permeabilization with PBS containing 0.1% Triton X-100 for 20 min at room temperature. The cells were blocked with 5% bovine serum albumin in PBS and reacted with a primary antibody targeting human extracellular E-cadherin (mouse mAb, Zymed Laboratories Inc.) or Calpain 2 (rabbit pAb, Cell Signaling) for 1 h at room temperature. After washing steps with PBS, the cells were incubated with Alexa Fluor 647-conjugated anti-mouse IgG (Molecular Probes) or Alexa Fluor 594-conjugated anti-rabbit IgG (Molecular Probes) for 1 h at room temperature, followed by incubation with Alexa Fluor 594-conjugated phalloidin. Finally, the coverslides were mounted onto glass slides using Vectashield mounting medium (Vector), and mounted samples were examined using a Zeiss LSM 510 confocal microscope system (version 3.2; Carl Zeiss). Images were obtained and processed with LSM 510 software. Three-dimensional reconstruction images were created from *z*-stack images using Imaris software (version 5.0; Carl Zeiss).

Construction and Screening of Tn916 Mutant Library—As a recipient strain, NIH35 with spontaneous resistance against streptomycin was generated by serial plating on THY agar containing 5% defibrinated sheep blood and streptomycin. Tn*916* insertional GAS mutants were generated by transposon mutagenesis using the Tn*916* donor strain *E. faecalis* CG110 (22). Briefly, the recipient and donor strains were grown to the mid-exponential phase and then mixed at a ratio of 25:1 and applied to a Hybond-N nylon membrane (0.2-μm pore size; GE Healthcare) placed on top of non-selective blood agar. After overnight incubation at 37 °C under a 5% CO_2 atmosphere, trans-conjugants were selected on THY agar plates containing 1 mg/ml streptomycin and 10 μg/ml tetracycline. A total of 1056 clones were pooled and applied to the above mentioned translocation assay.

To identify the gene disrupted by Tn*916*, genomic DNA from selected Tn*916* mutants was digested with HindIII, self-ligated, and used as a template for inverse PCR. The outward-reading primers sqTn916up1, sqTn916up2, sqTn916dw1, and sqTn916dw2 (supplemental Table S1) were used for the PCR assays. Amplicons containing the sequence flanking Tn*916* were cloned into a pGEM-T vector (Promega). The sequences of the Tn*916* insertion sites were determined using an ABI PRISM 310 genetic analyzer (Applied Biosystems) with conventional M13 primers (supplemental Table S1) and BigDye terminator chemistry. The data were then analyzed using BLASTN algorithms (see the NCBI Web site).

Immunoblotting—Caco-2 cells and HaCaT cells were seeded at 2×10^5 cells/well (35-mm diameter; Nunc) and cultured for 3 days and then infected with GAS strains at an MOI of 10. To remove non-adherent bacteria, the medium was replaced at 2 h after infection. At the end of the infection period, the infected cells were immediately washed with PBS and lysed with Laemmli gel loading buffer containing 6% 2-mercaptoethanol, and then the cell lysates were separated by SDS-PAGE and blotted onto polyvinylidene difluoride membranes. The membranes were blocked with Block Ace solution (Yukijirushi), followed by incubation with a primary antibody against human occludin (rabbit pAb, Zymed Laboratories Inc.), E-cadherin (mouse mAb, Zymed Laboratories Inc.), or β-actin (rabbit pAb, Cell Signaling) for 1 h at room temperature. The membranes were then washed with PBS and incubated with horseradish peroxidase-conjugated secondary antibody (Cell Signaling) for 1 h at room temperature. Following washing steps, the membranes were developed with ECL plus Western blot reagents (Amersham Biosciences). Intensity analysis of the protein bands was performed using Scion Image 4.0.3.2 software (Scion).

Real-time RT-PCR Assay—Three independent total RNA samples were prepared from wild type and *sagA* mutant strains grown to the late exponential phase. Synthesis of cDNA from total RNA was conducted with a SuperScript™ III first strand synthesis system for RT-PCR (Invitrogen). The possibility of DNA contamination was excluded by PCR analysis with non-reverse transcribed samples. Primer sets for selected genes were designed using Primer Express software (version 3.0; Applied Biosystems). All primers are listed in supplemental Table S1. The RT-PCR amplifications were performed using the SYBR Green method with an ABI StepOne™ real-time PCR system (version 2.2; Applied Biosystems). Relative expression amounts were calculated by the $\Delta\Delta C_T$ method. The level of *gyrA* expression was used as an internal control.

Paracellular Flux of FITC-dextrans—Caco-2 cells were grown on Millicell filters and infected with GAS at an MOI of 10 for 2 h. To remove non-adherent bacteria, the medium in the upper chamber was replaced with fresh medium at 2 h after infection. After removing non-adherent bacteria, FITC-dextran with a molecular mass of 4, 10, or 70 kDa (Sigma) was added to the apical surface of the cell monolayers. At 6 h after infection, the amount of FITC-dextran in the basolateral medium was measured using a Wallac 1420 ARVOsx fluorometer (excitation, 485 nm; emission, 535 nm; PerkinElmer Life Sciences).

RNA Interference—Predesigned Stealth Select siRNAs against calpain 1 (catalogue numbers HSS101345, HSS188701, and HSS188702) and calpain 2 (catalogue numbers HSS101347, HSS101348, and HSS188705) and negative controls (catalogue number 12935-112) were purchased from Invitrogen. Caco-2 cells were transfected with a single siRNA duplex for calpain 1 (catalogue number HSS101345) and calpain 2 (catalogue number HSS188705) at a final concentration of 50 nM. HaCaT cells were transfected with three siRNA duplexes targeting different regions of calpain 1 or calpain 2 genes at a final concentration of 150 nM. Transfection of siRNA was carried out using an Amaxa Nucleofector according to the manufacturer's instructions.

Lactate Dehydrogenase (LDH) Assay—Caco-2 and HaCaT cells were seeded at 2×10^5 cells/well (35-mm diameter; Nunc) and cultured for 3 days and then infected with GAS strains at an MOI of 10. To remove non-adherent bacteria, the medium was replaced 2 h after infection. At 6 or 8 h after infection, the release of LDH into the supernatant was analyzed using a CyTox 96 kit (Promega), according to the manufacturer's instructions. The percentage of cytotoxicity was calculated as LDH released in tested sample (A_{490})/maximum LDH release (A_{490}) $\times$ 100. Maximum release was determined as the amount released by total lysis of uninfected cells with 0.1% Triton X-100.

Annexin V and Propidium Iodide Staining—Caco-2 cells and HaCaT cells were seeded at 2×10^5 cells/well onto coverslides pretreated with poly L-lysine (13-mm diameter; Matsunami) and cultured for 3 days at 37 °C under a 5% CO_2 atmosphere. The cells were infected with strain NIH35 at an MOI of 10. After washing steps with annexin V binding buffer (10 mM HEPES (Dojindo), 140 mM NaCl (Wako), and $CaCl_2$ (Wako), pH 8.0), the cells were incubated with annexin V binding buffer for 15 min at 37 °C under a 5% CO_2 atmosphere and then stained with annexin V-FITC reagent (BioVision) and propidium iodide (Molecular Probes) for 5 min at room temperature, followed by fixation with 4% paraformaldehyde in PBS for 10 min. Cell nuclei were stained with DAPI (Molecular Probes). Finally, the coverslides were mounted onto glass slides using VECTASHIELD mounting medium (Vector), and mounted samples were examined using a Zeiss LSM 510 confocal microscope system, version 3.2 (Carl Zeiss). Images were obtained and processed with AxioVision software (version 4.6; Carl Zeiss).

Statistical Analysis—Statistical analysis was performed using a Mann-Whitney *U* test. A confidence interval with a p value of <0.05 was considered to be significant.

RESULTS

Capsule Production Is Crucial for GAS Translocation across Epithelial Barrier in a Strain-specific Manner—As a first step toward understanding the mechanism by which GAS translocates across the epithelial barrier, we examined whether bacterial capsule production is a prerequisite for the process. GAS colonizes human pharyngeal epithelia and keratinocytes; thus, filter-grown human keratinocyte HaCaT cells were initially tested for suitability as a model of the epithelial barrier. However, the integrity of the junctions, as confirmed by TER, was not stable for initial screening of GAS translocation. On the other hand, human intestinal epithelial Caco-2 cells express typical epithelial markers of differentiation and have been widely used (23). Therefore, to ensure the integrity of the experimental intercellular junction, Caco-2 cells, with a peak TER value of 450–500 ohms·cm^2, were grown in a Millicell filter system and utilized for the translocation assays as an epithelial barrier model. Four GAS serotype strains recovered from invasive disease, serotype M1 strain SSI-9, serotype M3 strain SSI-1, serotype M12 strain 30, and serotype M28 strain NIH35, were used to infect the apical surface of Caco-2 monolayers, and then translocation across the monolayers was monitored for up to 6 h at 2-h intervals. Isogenic acapsulated *hasA* mutant strains were also tested under the same conditions. For all tested strains, the rates of translocated bacteria in the inoculum dose were less than 0.01% of the inoculum until 6 h after infection (data not shown). Thereafter, strains SSI-1 and 30 were detected in basolateral medium below the membrane support, demonstrating migration of the bacteria through the monolayers (Fig. 1*A*). In contrast, the translocation ability of their acapsulated mutants was abrogated, which supports a previously reported function of the capsule (16). Despite the fact that capsule production by NIH35 was relatively low (Fig. 1*B*), marked translocation was observed. We also noted that translocation efficiency did not differ between strain NIH35 and its acapsulated strain (Fig. 1*A*). On the other hand, neither strain SSI-9 nor the acapsulated mutant was capable of translocating across the monolayer. An antibiotic protection assay revealed that strain SSI-9 tends to internalize into an intracellular niche (supplemental Fig. S1).

To examine whether the Caco-2 model system is adequate to assess GAS translocation, the translocation ability of GAS strains was also tested using filter-grown HaCaT cells, with the integrity examined by assessing the permeability to fluorescein (see "Experimental Procedures"). As expected, similar findings were obtained with HaCaT cells (data not shown). Taken together, our results suggest that capsule-dependent translocation is a serotype-specific or even strain-specific event. Consequently, we hypothesized that an additional factor besides the capsule plays a critical role in the translocation process.

Identification of Additional Bacterial Factor Associated with Translocation—Because we confirmed that strain NIH35 was able to translocate across epithelial cells irrespective of capsule production, we randomly mutagenized the strain with Tn*916* to search for alternative bacterial factors that contrib-

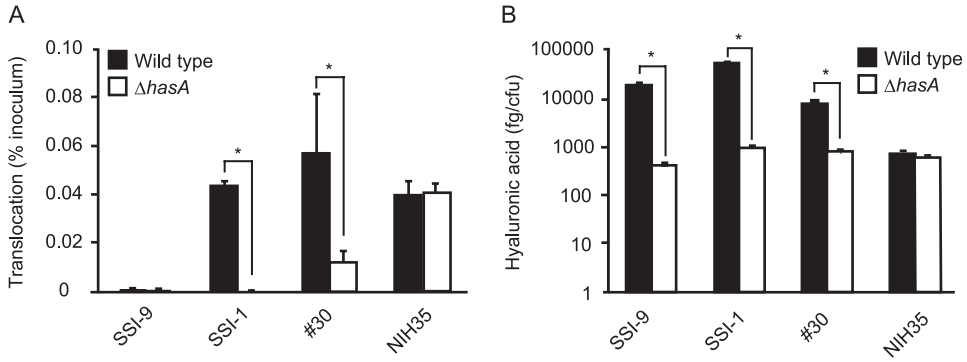

FIGURE 1. **The capsule is not the sole bacterial factor for translocation across epithelial cells.** *A*, Caco-2 cells were grown using a Millicell system and then infected with GAS clinical isolates and isogenic acapsular mutants at an MOI of 10 for 2 h. After removing non-adherent bacteria, the ability of the GAS strains to translocate across epithelial cells at 6 h after infection was assessed by quantitative cultures of medium obtained from the lower chambers. Three experiments were performed, and data are presented as the mean ± S.D. (*error bars*) of sextuplet samples from a representative experiment. *, $p < 0.01$. *B*, the level of capsule production on the cell surface was measured using an enzyme-linked immunosorbent assay. Data shown are represented as the mean ± S.D. of sextuplet samples from a representative experiment. *, $p < 0.01$.

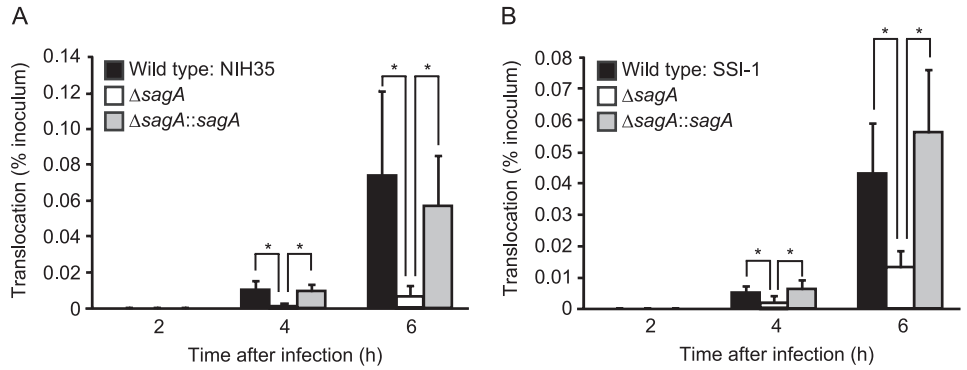

FIGURE 2. **SLS is involved in translocation of GAS across epithelial cells.** Caco-2 cells were grown on Millicell filters and then infected with GAS strains at an MOI of 10 for up to 6 h. *A* and *B*, bacterial translocation is expressed as a percentage of bacteria recovered from medium beneath the monolayer at the indicated time of infection of the apical surface with wild type, the *sagA* deletion mutant, or the complemented strain. Shown are results of translocation rates of strains NIH35 (*A*) and SSI-1 (*B*). All experiments were performed in sextuplet with three technical repeats. Data shown are presented as the mean ± S.D. (*error bars*) of six wells from a representative experiment. *, $p < 0.01$.

ute to the translocation phenotype. Approximately 1,000 mutants were isolated and subjected to translocation assays, which found 18 mutants with significantly reduced translocation ranging from 70 to 90%. Subsequently, the transposon insertion sites in those strains were determined. Interestingly, in some of the mutants that showed the lowest translocation efficiency, Tn*916* was located in the promoter region of the *sagA* gene, which encodes SLS, responsible for β-hemolysis. In fact, the *sagA*::Tn*916* mutants demonstrated no β-hemolysis on blood agar, indicating that SLS activity had been ablated. Additional tests demonstrated an apparent difference in the efficiency of translocation between the wild type and the *sagA*::Tn*916* mutant (data not shown), suggesting that SLS enables GAS to penetrate the epithelial barrier.

SLS Contributes to Translocation of GAS across Epithelial Barrier—Because the *sagA*::Tn*916* mutant contains a transposon insertion in the promoter region yet retains the intact structural gene, we constructed an in-frame *sagA* deletion mutant and its complemented strain to verify the requirement of SLS for GAS translocation. Growth of the wild type and mutant strains (data not shown) as well as their capacity to adhere to the apical surface of the Caco-2 monolayers were nearly identical (supplemental Fig. S2*A*). In addition, the amount of hyaluronic acid was not changed by the mutation or subsequent complementation of the *sagA* gene (supplemental Fig. S2*B*). Furthermore, we investigated whether mutations in the *sagA* locus could be associated with alterations in virulence gene expression (24–26). Our in-frame *sagA* deletion mutant in an M28 background was free of polar effects on the downstream genes (*i.e. sagB* to *-I*, which encode proteins responsible for modification and secretion of SLS), and we did not observe significant difference in the expression of the *emm*, *mga*, *speB*, and *slo* genes encoding M protein, a stand-alone global regulator, cysteine protease, and cholesterol-dependent cytolysin, respectively (data not shown). Nevertheless, deletion of the *sagA* gene compromised the ability of GAS to translocate across the Caco-2 monolayers (Fig. 2*A*), whereas the translocation efficiency of the complemented strain was partially restored to the level of the wild type. These results indicate that SLS is not involved in eukaryotic adhesion but is rather a crucial factor for facilitating GAS translocation. To further investigate the generality of the role of SLS in the translocation process, we also constructed a *sagA* deletion mutant and its complemented strain with a background of the serotype M3 strain SSI-1, which has a relatively high level of capsule production (Fig. 1*B*). Although deletion of the *sagA* gene had no effect on capsule production (Fig. S2*B*), translocation of the *sagA* mutant was decreased by

~70% and completely recovered by complementation of the *sagA* gene (Fig. 2*B*). Together with the previous results demonstrating that the translocation is abolished by the *hasA* mutation (Fig. 1*A*), it was suggested that the GAS translocation process is a multifactorial event.

Of note, SLS possesses cytotoxic effects against various types of eukaryotic cells, including epithelial cells (27, 28). Thus, we examined release of the cytoplasmic enzyme LDH into cell culture medium to elucidate the possible cytotoxic effects of SLS on Caco-2 cells and HaCaT cells. LDH release was not induced following infection with any of the tested strains under the experimental conditions used (supplemental Fig. S3*A*). Moreover, staining with annexin V and propidium iodide also revealed no apparent apoptotic or necrotic cellular events in Caco-2 cells and HaCaT cells infected with strain NIH 35 (supplemental Fig. S3*B*). Therefore, we consider that translocation of GAS across epithelial cells is not attributable to either a cytotoxic effect of SLS or other bacterial traits.

SLS Is a Bacterial Determinant for GAS-induced Cleavage of Intercellular Junctions—Loss of integrity of intercellular junctions is expected to reduce the barrier function of monolayers, as reflected by the decrease in TER (reviewed in Refs. 29 and 30). Caco-2 cell monolayers infected with the *sagA* mutant exhibited a delayed decrease of TER, as compared with those infected with the wild type and revertant strain (Fig. 3*A*, 6 h postinfection). We also tested effect of the *sagA* deletion on the junctional integrity using a biochemical assay that measured transepithelial transport of FITC-labeled dextrans (supplemental Fig. S2*C*). Consistent with the TER assay, passive diffusion of dextrans across the cell monolayers was decreased in cells infected with the *sagA* mutant, as compared with those infected with the wild type strain. These results prompted us to evaluate the possible involvement of SLS in GAS-induced cleavage of intercellular junctions. In fact, cleavage of occludin and E-cadherin in both Caco-2 cells and HaCaT cells infected with the wild type was detected with antibodies against the extracellular domains of occuludin and E-cadherin (Fig. 3*B*). Interestingly, cleavage of the full-length forms of occludin and E-cadherin, which are recognized as a 60 kDa band and 120/100 kDa bands, respectively, was markedly hampered by the *sagA* mutation, whereas it was completely restored by the complementation. A distinct cleavage product of occludin with an apparent molecular mass of about 50 kDa was detected in Caco-2 cells infected with the wild type and those with the complemented strain; however, it was not detected in cells infected with the *sagA* mutant and in non-infected cells, which suggests that the 50-kDa fragment is an SLS-induced cleavage product of occludin. However, a 50-kDa fragment reacting with the anti-occludin antibody was detected in all of the tested samples of HaCaT cells. On the other hand, the cleavage of JAM-1, a member of the group of TJ proteins, was not detected in cells infected with any of the strains (data not shown). These findings indicate that SLS induces the destabilization and opening of specific intercellular junctions, either directly or indirectly. Thus, defects in epithelial integrity may facilitate the translocation of GAS across the epithelial barrier.

Proinflammatory cytokines, such as TNF-α, IFN-γ, and IL-1β, have disruptive effects on the TJ barrier (31–33); thus, we examined the release of cytokines from monolayers infected with GAS strains using an ELISA (data not shown). However, remarkable cytokine release could not be detected in our model during the period of the translocation assay, which suggests that destabilization of the junctions is not due to a cytokine effect.

SLS Contributes to Translocation of GAS via Intercellular Junctions—To visualize the effect of *sagA* deletion on the translocation process, Caco-2 cells were infected with EGFP-expressing GAS strains and analyzed using confocal microscopy. An association of GAS with the perimeter of the Caco-2 cells was observed in those infected with either the wild type or the *sagA* mutant at 6 h after infection (Fig. 4*A*). Observations of the *z*-sections clearly indicated decreased fluorescent intensity for E-cadherin at the apical site of cells infected with the wild type strain but not in those infected with the *sagA* mutant. Optical sections of the infected cells stained for E-cadherin as a *blue image* were used to reconstruct three-dimensional images (Fig. 4*B*), which revealed that the cleavage of E-cadherin developed around the bacterial translocation site in the cells infected with wild type strain. On the other hand, the *sagA* mutant was mainly found on the apical surface of intact E-cadherin. Based on these results, we speculated that SLS is a crucial bacterial factor for GAS invasion into deeper tissue, which is followed by degradation of intercellular junctions associated with the epithelial barrier.

Involvement of Cellular Cysteine Protease in Translocation across Epithelial Cells—Our results led us to speculate that SLS contributes to paracellular translocation of GAS by inducing degradation of membrane-spanning junctional proteins, such as occludin and E-cadherin. However, it is not conceivable that SLS possesses a proteolytic activity to directly cleave the junctional proteins. Very recently, it was reported that calpain, a host cysteine protease activated by *Pseudomonas aeruginosa* infection or TLR2 signaling, cleaves both occludin and E-cadherin to promote recruitment of polymorphonuclear leukocytes into airway epithelial cells (34). To investigate the potential contribution of calpain to GAS translocation, the calpain inhibitors calpeptin and ALLN were utilized (Fig. 5*A*). The ability of both the wild type and the complemented strain to translocate across Caco-2 monolayers was significantly inhibited in the presence of calpain inhibitors, whereas those inhibitors did not affect translocation of the *sagA* mutant. Treatment with either calpeptin or ALLN also inhibited the decrease of TER in Caco-2 cells infected with the wild type and the complemented strain but not in those infected with the *sagA* mutant (Fig. 5*B*). On the other hand, MG-115, a proteasome inhibitor, had no effect on both GAS translocation and the decrease of TER. These results suggest that calpain participates in SLS-induced translocation of GAS across an epithelial barrier.

GAS-induced Cleavage of Intercellular Junctions Is Associated with Membrane Recruitment of Calpain—It is known that calpain cleaves a cytoplasmic domain of E-cadherin,

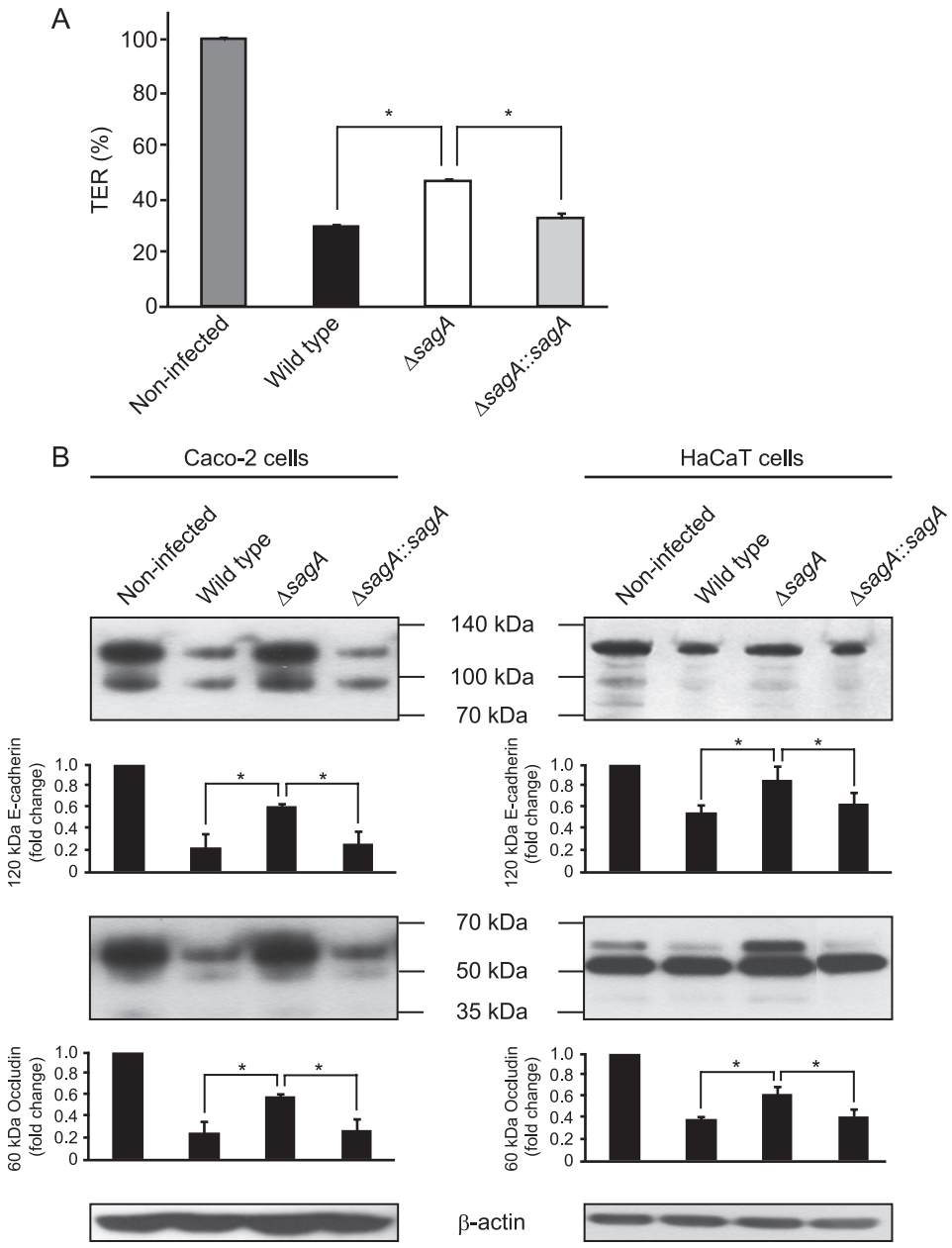

FIGURE 3. **SLS is related to GAS-induced destabilization of intercellular junctions.** *A*, Caco-2 cells were grown on Millicell filters and then infected with NIH35 strain, the *sagA* deletion mutant, or the complemented strain. After 6 h of infection, the reduction in TER was measured. The TER value of non-infected cells was set at 100%. Data are represented as the mean ± S.D. (*error bars*) of sextuplet samples from a representative experiment. *, $p < 0.01$. *B*, Caco-2 and HaCaT cells were infected with strain NIH35, the *sagA* deletion mutant, or the complemented strain at an MOI of 10 for 6 or 8 h, respectively. Cleavage of E-cadherin and occludin was detected in whole cell lysates by Western blot analysis as described under "Experimental Procedures." β-Actin served as a loading control. The graphs *below* the representative blot show -fold change of E-cadherin and occludin normalized to β-actin. The intensity of the bands was quantified using Scion Image. Data are represented as the mean ± S.D. of three independent experiments. *, $p < 0.05$.

resulting in partial disruption of cellular adhesion (35). To study the involvement of calpain in GAS-induced cleavage of E-cadherin, Caco-2 cells and HaCaT cells were pretreated with calpeptin and then subsequently infected with the wild type strain. We utilized an antibody against the cytoplasmic domain of E-cadherin to detect the E-cadherin full-length form as a single band. Pretreatment of both types of cells with increasing concentrations of calpeptin blocked cleavage of E-cadherin full-length form in a dose-dependent manner (Fig. 6*A*). To further address the role of cellular calpain in GAS infection, the expression of calpain 1 or 2 was silenced by siRNA. The results of Western blot analysis showed that calpain 1 or calpain 2 was effectively knocked down by transfection of siRNA into Caco-2 cells and HaCaT cells (Fig. 6*B*). Cleavage of the E-cadherin full-length form was detected in Caco-2 cells transfected with scrambled control oligonucleotides but not in cells transfected with calpain 1 or calpain 2 siRNA (Fig. 6*C*). Inhibition of E-cadherin cleavage was also found in HaCaT cells transfected with calpain 1 or calpain 2 siRNA. Finally, we investigated the expression of calpain 2 in HaCaT cells infected with EGFP-expressing GAS strains using confocal

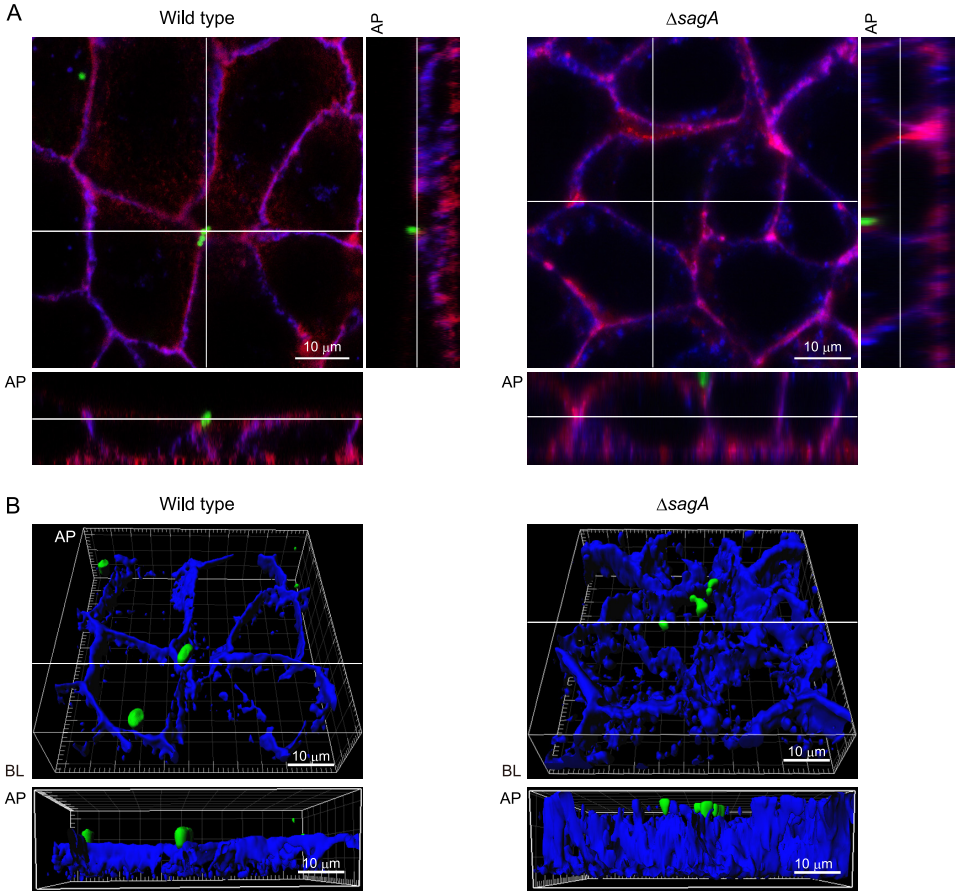

FIGURE 4. **SLS contributes to GAS translocation via a paracellular route.** *A*, Caco-2 cells were infected with EGFP-expressing GAS strains as *green images* at an MOI of 10 for 6 h. Extracellular E-cadherin was labeled with anti-E-cadherin and Alexa Fluor 647-conjugated antibodies as *blue images*, whereas F-actin was labeled with Alexa Fluor 594-conjugated phalloidin as *red images*. GAS-infected cells were analyzed using a confocal laser-scanning microscope, and *z*-slices were taken at 0.5-μm intervals. The *bottom* and *side strips* at the *white lines* drawn in the *main panel* are *z*-sections. *B*, three-dimensional immunofluorescent images of GAS-infected Caco-2 cells were reconstructed from confocal optical sections obtained in *A*, using Imaris software. The *lower panels* show the *z*-sections at the *white line* drawn in the *top panel* three-dimensional images. Data shown are representative of at least three separate experiments. *AP*, apical; *BL*, basolateral.

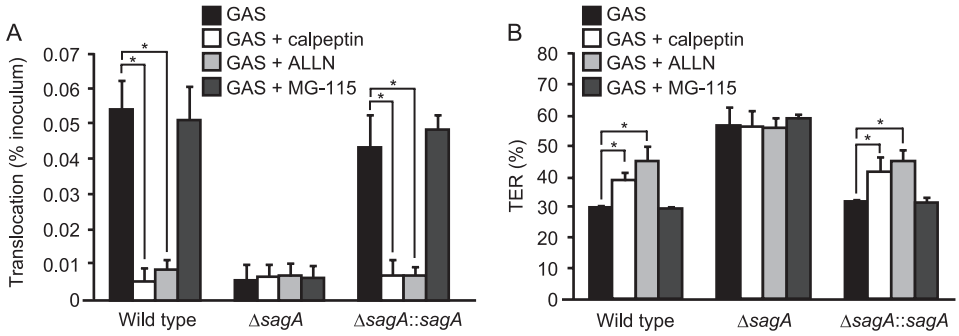

FIGURE 5. **Involvement of calpain in SLS-induced GAS translocation across epithelial cells.** *A*, Caco-2 cells were grown on Millicell filters and then treated with 50 μM calpeptin, 20 μM ALLN, or 30 μM GM-115 for 1 h. Thereafter, cell monolayers were infected with strain NIH35, the *sagA* mutant, or the complemented strain at an MOI of 10. Bacterial translocation across the cells was determined at 6 h after infection. *B*, effects of proteolysis inhibitors on reduction in TER in cells infected with GAS strains for 6 h. The TER value of non-infected cells was set at 100%. All experiments were performed in sextuplet with three technical repeats. Data are presented as the mean ± S.D. (*error bars*) of six wells from a representative experiment. *, $p < 0.01$.

microscopy (Fig. 6*D*). The confocal images showed that calpain was widely distributed within the cytoplasm of non-infected cells. At 2 h after infection, calpain was colocalized with peripheral E-cadherin in cells infected with the wild type but not in those infected with the *sagA* deletion mutant. These results indicate that GAS recruits calpains to the plasma membrane by an unidentified SLS function during the early stage of infection and then utilizes proteolytic activity to invade into deeper tissue via a paracellular route.

DISCUSSION

GAS has traditionally been viewed as an extracellular pathogen responsible for human diseases that occur in various anatomical tissues. A previous study reported that cell signaling triggered by interactions of the GAS capsule with

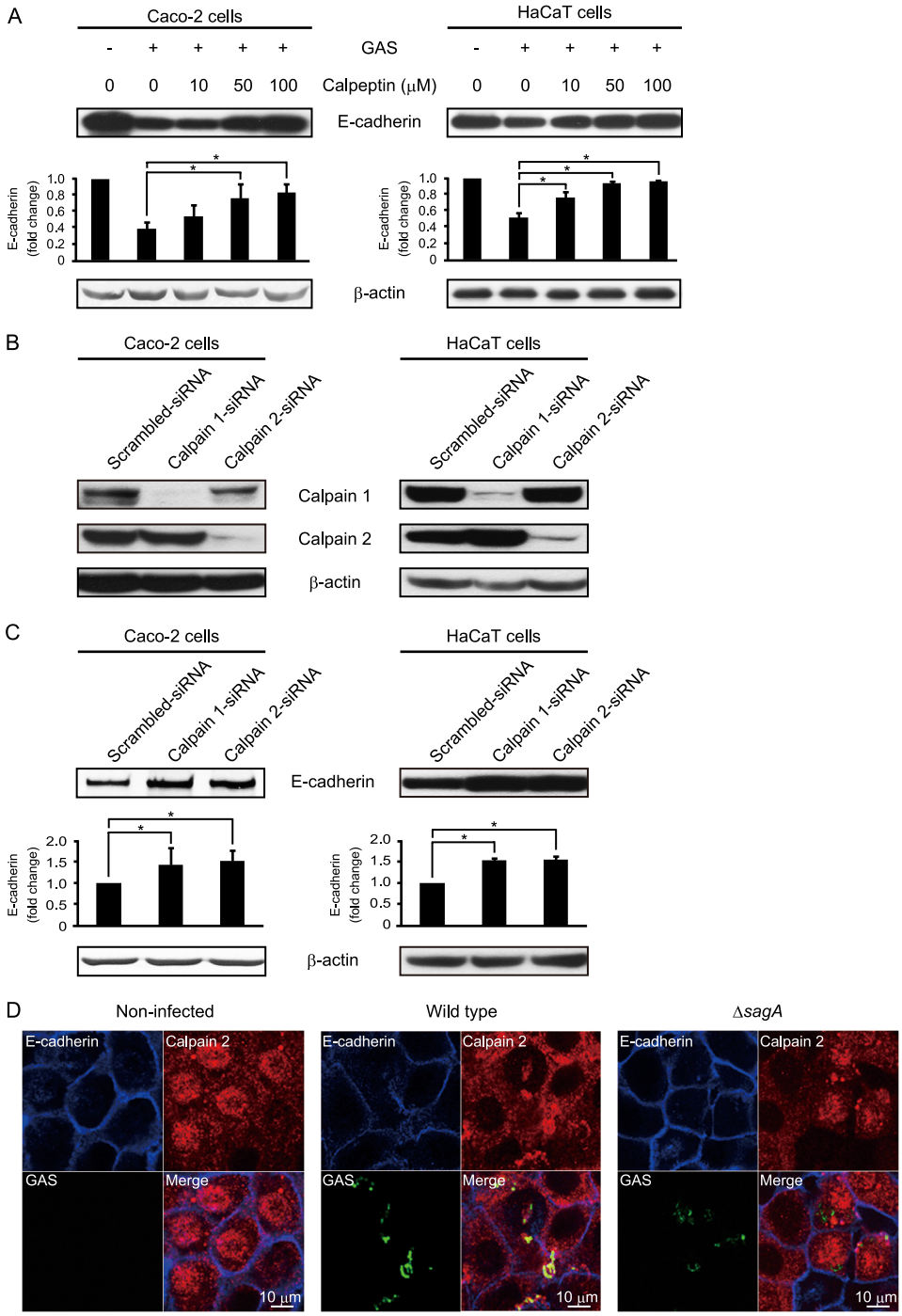

FIGURE 6. **Calpain is involved in GAS-induced disruption of intercellular junctions.** *A*, Caco-2 and HaCaT cells were pretreated with various concentrations of calpeptin for 1 h and then infected with strain NIH35 at an MOI of 10 for 6 or 8 h. Whole cell lysates were subjected to Western blot analysis using anti-E-cadherin and anti-β-actin antibodies. β-Actin served as a loading control. The graphs *below* the representative blot show -fold change of E-cadherin normalized to β-actin. The intensity of the bands was quantified using Scion Image. Data are represented as the mean ± S.D. (*error bars*) of three independent experiments. *, $p < 0.05$. *B*, Caco-2 and HaCaT cells were transfected with calpain 1-targeted or calpain 2-targeted siRNA. A scrambled siRNA was utilized as a negative control. At 48 h after transfection, whole cell lysates were subjected to Western blot analysis using anti-calpain 1 and anti-calpain 2 antibodies. β-Actin served as a loading control. *C*, Caco-2 and HaCaT cells were transfected with calpain 1-targeted or calpain 2-targeted siRNA. A scrambled siRNA was utilized as a negative control. At 48 h after transfection, cells were infected with strain NIH35 at an MOI of 10 for 5 or 7 h. Cleavage of E-cadherin was detected in cell lysates by Western blot analysis using anti-E-cadherin and anti-β-actin antibodies. β-Actin served as a loading control. The graphs *below* the representative blot show -fold increase of E-cadherin normalized to β-actin. The intensity of the bands was quantified using Scion Image. Data are represented as the mean ± S.D. of three independent experiments. *, $p < 0.05$. *D*, HaCaT cells were infected with EGFP-expressing GAS strains at an MOI of 10 for 2 h. Extracellular E-cadherin was labeled with anti-E-cadherin and Alexa Fluor 647-conjugated antibodies as *blue images*, whereas calpain 2 was labeled with Alexa Fluor 594-conjugated antibodies as *red images*. GAS-infected cells were analyzed using a confocal laser-scanning microscope. Data shown are representative of at least three separate experiments.

CD44 on host cells opened intercellular junctions and promoted tissue penetration of GAS through a paracellular route (16). Based on our findings with various serotype strains and their respective acapsular strains, we demonstrated that capsule production was not commonly correlated with the ability to translocate across an epithelial monolayer, which

prompted us to search for other GAS molecules that cause bacterial translocation. As a result, we found SLS to be a crucial alternative factor for bacterial translocation.

The *sagA* gene is a structural gene for SLS that encodes a 53-amino acid precursor of a bacteriocin-like toxin and is enzymatically processed and modified by downstream gene products (20, 36–39). SLS is also an oxygen-stable and nonimmunogenic hemolysin with a broad cytolytic spectrum (27), which exists primarily in cell-bound form and is delivered most effectively to target cells by direct contact with GAS (40). *In vitro* studies have suggested that SLS contributes to pathogenesis by direct cytotoxicity and inhibition of neutrophil phagocytosis (28), whereas it is also known to manipulate inflammatory host response during the early stages of infection (25, 38). In addition, the expression of SLS promotes virulence in murine models of invasive infection (28, 41, 42). Thus, several lines of evidence clearly show the involvement of SLS in the pathogenesis of GAS-related diseases.

In our experiments with a serotype M28 strain, we found that in-frame deletion of the *sagA* gene compromised the ability of GAS to translocate across epithelial monolayers, which was also seen with a highly encapsulated M3 strain, indicating that the contribution of SLS is universal among the species. Because the translocation phenotype of the M3 strain was abrogated without capsule production, it is possible that the translocation step is under collaborative control of several bacterial factors; otherwise, it would probably occur in a serotype- or strain-specific manner. Additional experiments are required to identify other bacterial factors responsible for GAS translocation. Moreover, because homologs of the *sag* operon have been identified in some species, including group C and G streptococci and *Streptococcus iniae*, it would be of interest to investigate whether the SLS-like hemolysin produced by other species also plays a crucial role in bacterial translocation across an epithelial barrier (39, 41, 43).

We initially speculated that translocation of GAS occurs via either a paracellular or intracellular route, and our findings confirmed that it mainly occurs via a paracellular route during the period of infection tested in this study. In order to translocate via an intracellular route, the most effective strategy is probably by inducing cell death to damage the epithelial barrier, which is also induced by extracellular GAS with an array of exotoxins, including SLS and the cytolysin-mediated translocation system (13, 14, 44). When we measured the amount of released LDH as a marker of cell injury during the translocation assay, it was not observed in epithelial cells exposed to either the wild type or the *sagA* deletion mutant. Therefore, the translocation phenotype of the wild type is not attributable to epithelial cell death induced by GAS.

An alternative scenario is that host response against bacterial adherence and internalization and/or host cell-associated bacteria directly modulate the integrity of intercellular junctions. Data obtained over the past decade indicate that GAS is capable of manipulating its own entry into epithelial cells (45). Although GAS internalization contributes to bacterial persistence despite antibiotic therapy (46), it is not clear whether it is linked with the ability of GAS to penetrate the epithelial barrier. Because introduction of the *sagA* deletion did not influence bacterial internalization or adherence in our model, we propose that SLS itself or other bacterial factors, whose expression or function is altered by the *sagA* deletion, promote bacterial translocation in combination with host factors. Due to the difficulties with preparing native or recombinant SLS (47), we could not test the direct effects of SLS on the translocation and interaction of SLS with intercellular junctions. Recently, Lee *et al.* (39) reported *in vitro* reconstitution of streptolysin S activity, which was prepared by mixing recombinant SagA and modifying enzymes. In a future investigation, the direct effects of SLS on the process of translocation may be elucidated by utilizing recombinant SLS prepared by methods described in that report.

Although it is not likely that SLS itself possesses proteolytic activities, we found that it mediates GAS-induced cleavage of intercellular junctional proteins, such as occludin and E-cadherin. We examined whether the ability of SLS to manipulate inflammatory response contributes to the phenotype because it has been proposed that proinflammatory cytokines induce a pathologic opening of the intestinal TJ barrier, allowing increased paracellular permeation of luminal agents, such as bacteria and other toxic substances (48). The disruptive actions against the TJ barrier by TNF-α, IFN-γ, and IL-1β have been well established (31–33), and release of cytokines, such as TNF-α, IFN-γ, IL-6, and IL-8, was observed in pharyngeal epithelial cells infected for 48 h with a serotype M49 GAS strain (49). In our experiments with the M28 GAS strain, we did not detect cytokine release into the culture medium during the period of infection. Thus, the cleavage of intercellular junctional proteins in our model was not due to the cytotoxic and inflammatory effects of SLS.

In addition to the cytotoxic effects of SLS, it is important to discuss regulation of its expression. The appropriate timing of SLS expression is probably critical at the initial stage of GAS infection. Tight control of *sagA* expression during infection might be achieved through integration of multiple regulators, including the CovRS (also called CsrRS) two-component system, FasBCAX, Mga, and RALPs (50). Notably, several investigations have found that the transition from local to systemic infection is linked to spontaneous mutations of *covRS* genes (51–53). Such mutations result in abrogating the repression of an array of genes encoding virulence factors, including SLS and the capsule (54–57). Hence, to examine the relationship between the *covRS* mutation and the ability of GAS to translocate across epithelial cells, we analyzed the chromosomal sequence of the *covRS* locus in several colonies of GAS that showed successful translocation. However, no mutation was detected (data not shown). Therefore, it is considered that *covRS* mutation may not occur during translocation, although it would be possible under the conditions GAS encounters *in vivo*.

Separate investigations have reported that various mutations in the chromosomal locus of the *sagA* gene could be associated with alterations in expression of other GAS virulence genes, including M protein, cysteine protease, and streptokinase (24–26). Consistent with several analyses of transposon insertional mutants in the *sagA* promoter region of M1 and M18 strains (20) and an in-frame *sagA* deletion

mutant in the background of a serotype M1 strain (28), we did not observe distinct effects of *sagA* deletion on the expression of M protein, cysteine protease, or streptolysin O at the transcriptional level in the serotype M28 in-frame *sagA* deletion mutant. We also confirmed that capsule production is not affected by *sagA* deletion. These findings indicate that the reduction in the ability of the *sagA* mutant to translocate into epithelial cells is not attributable to pleiotropic effects caused by *sagA* deletion.

Given the preferential translocation of GAS via a paracellular route, it is intriguing to speculate that GAS may be guided to intercellular junctions by unidentified surface-displayed GAS proteins. The human pathogen group B streptococcus possesses genetically distinct β-hemolysin and also translocates across the epithelial barrier via a paracellular route, and it was recently proposed that the pili backbone protein contributes to its paracellular translocation (17). However, no involvement of pili in GAS translocation was observed in the present M28 GAS strain (data not shown). Based on our findings that both the wild type and the *sagA* deletion mutant became localized in intercellular space, other factors in addition to SLS may participate in bacterial localization.

We also found evidence of calpain involvement in GAS translocation. Recently, Chun *et al.* (34) proposed that TLR-dependent Ca^{2+} fluxes function as signals for the activation of calpains, which subsequently target junctional proteins, and also demonstrated that calpains cleave specific junctional proteins, such as occludin and E-cadherin. Calpains are ubiquitously expressed as Ca^{2+}-dependent protease. However, when associated with the membrane, the requirement for Ca^{2+} is diminished to a more physiological range because it occurs when calpains are mobilized to the epithelial junction (58). Consistent with TLR2-induced signaling, membrane recruitment of calpain and specific cleavage of occludin and E-cadherin were observed in cells infected with a GAS wild type strain in the present study. It is also known that a 100-kDa truncated fragment of E-cadherin is generated by calpain in epithelial cells (35, 59). In the present study, a 100-kDa polypeptide reacting with the antibody against the extracellular domain of E-cadherin was detected in both non-infected cells and cells treated with the calpain inhibitor calpeptin (data not shown). Therefore, the 100-kDa form of E-cadherin detected in cells infected with any GAS strain may not be a calpain-dependent proteolytic fragment. Interestingly, although a previous report indicated that calpain targets the N-terminal portion of occludin and induces the appearance of a 45-kDa cleavage fragment in airway cells (34), we detected a 50-kDa cleavage fragment in GAS-infected Caco-2 cells in an SLS-dependent manner. However, this fragment was clearly detected even in non-infected HaCaT cells, which may reflect the relatively low integrity of tight junctions. Due to the high background of the 50 kDa band, we could not detect the SLS-dependent cleavage pattern as observed in Caco-2 cells. These results suggest that either calpain itself or an alternative calpain-activated factor is involved in GAS-induced cleavage of intercellular junctions. Based on findings showing that GAS translocation and destabilization of junctions were inhibited by a pharmacological calpain inhibitor or genetic interference with calpain, we speculate that SLS signals the activation of calpains and augments GAS translocation across the epithelial barrier.

Our data also imply that SLS facilitates penetration of bacterial extracellular molecules into deeper tissues via degradation of epithelial intercellular junctions in concert with the host protease calpain. Indeed, passive diffusion of FITC-dextran, which has a molecular mass of 70 kDa, across cell monolayers was observed in those infected with the wild type strain. Therefore, we speculate that various virulence factors, including streptokinase (~50 kDa), cysteine protease (28.5 kDa), and superantigenic toxins (24–28 kDa), penetrate following the opening of paracellular junctions and initiate various immune responses responsible for such diseases as necrotizing fasciitis and streptococcal toxic shock syndrome.

In summary, we report a novel biological aspect of SLS associated with mediation of GAS transepithelial migration. Furthermore, our results indicate that epithelial calpains may play a critical role in the cleavage of intercellular junctions. We propose that SLS mediates calpain activation during the translocation process along with degradation of intercellular junctions. Although many questions remain to be answered, understanding of how the SLS-induced signaling pathway of calpain activation occurs may provide new avenues for comprehension of the interactions between host cells and GAS at the initial stages of invasive infections.

Acknowledgments—We thank H. Watanabe and T. Murai for providing GAS strains. We acknowledge N. Fusenig and R. Steubing for the HaCaT cell line. The pAT18 plasmid was kindly provided by P. Trieu-Cuot. We gratefully acknowledge T. Sekizaki and D. Takamatsu for the pSET4s plasmid. We thank C. Matsumura for helpful technical assistance.

REFERENCES

1. Hartsock, A., and Nelson, W. J. (2008) *Biochim. Biophys. Acta* **1778,** 660–669
2. Balkovetz, D. F., and Katz, J. (2003) *Microbe Infect.* **5,** 613–619
3. Sousa, S., Lecuit, M., and Cossart, P. (2005) *Curr. Opin. Cell Biol.* **17,** 489–498
4. Matsumura, T., Jin, Y., Kabumoto, Y., Takegahara, Y., Oguma, K., Lencer, W. I., and Fujinaga, Y. (2008) *Cell Microbiol.* **10,** 355–364
5. Cunningham, M. W. (2000) *Clin. Microbiol. Rev.* **13,** 470–511
6. Carapetis, J. R., McDonald, M., and Wilson, N. J. (2005) *Lancet* **366,** 155–168
7. Carapetis, J. R., Steer, A. C., Mulholland, E. K., and Weber, M. (2005) *Lancet Infect. Dis.* **5,** 685–694
8. Terao, Y., Kawabata, S., Kunitomo, E., Murakami, J., Nakagawa, I., and Hamada, S. (2001) *Mol. Microbiol.* **42,** 75–86
9. Terao, Y., Kawabata, S., Nakata, M., Nakagawa, I., and Hamada, S. (2002) *J. Biol. Chem.* **277,** 47428–47435
10. Bisno, A. L., Brito, M. O., and Collins, C. M. (2003) *Lancet Infect. Dis.* **3,** 191–200
11. Joh, D., Wann, E. R., Kreikemeyer, B., Speziale, P., and Höök, M. (1999) *Matrix Biol.* **18,** 211–223
12. Kawabata, S., Kuwata, H., Nakagawa, I., Morimatsu, S., Sano, K., and Hamada, S. (1999) *Microb. Pathog.* **27,** 71–80
13. Nakagawa, I., Nakata, M., Kawabata, S., and Hamada, S. (2001) *Cell Microbiol.* **3,** 395–405
14. Cywes Bentley, C., Hakansson, A., Christianson, J., and Wessels, M. R. (2005) *Cell Microbiol.* **7,** 945–955

15. Klenk, M., Nakata, M., Podbielski, A., Skupin, B., Schroten, H., and Kreikemeyer, B. (2007) *ISME J.* **1,** 678–692
16. Cywes, C., and Wessels, M. R. (2001) *Nature* **414,** 648–652
17. Pezzicoli, A., Santi, I., Lauer, P., Rosini, R., Rinaudo, D., Grandi, G., Telford, J. L., and Soriani, M. (2008) *J. Infect. Dis.* **198,** 890–898
18. Trieu-Cuot, P., Carlier, C., Poyart-Salmeron, C., and Courvalin, P. (1991) *Gene* **102,** 99–104
19. Takamatsu, D., Osaki, M., and Sekizaki, T. (2001) *Plasmid* **46,** 140–148
20. Betschel S. D., Borgia, S. M., Barg, N. L., Low, D. E., and De Azavedo, J. C. (1998) *Infect. Immun.* **66,** 1671–1679
21. Lin, A., Loughman, J. A., Zinselmeyer, B. H., Miller, M. J., and Caparon, M. G. (2009) *Infect. Immun.* **77,** 5190–5201
22. Nida, K., and Cleary, P. P. (1983) *J. Bacteriol.* **155,** 1156–1161
23. Mariadason, J. M., Arango, D., Corner, G. A., Arañes, M. J., Hotchkiss, K. A., Yang, W., and Augenlicht, L. H. (2002) *Cancer Res.* **62,** 4791–4804
24. Li, Z., Sledjeski, D. D., Kreikemeyer, B., Podbielski, A., and Boyle, M. D. (1999) *J. Bacteriol.* **181,** 6019–6027
25. Biswas, I., Germon, P., McDade, K., and Scott, J. R. (2001) *Infect. Immun.* **69,** 7029–7038
26. Mangold, M., Siller, M., Roppenser, B., Vlaminckx, B. J., Penfound, T. A., Klein, R., Novak, R., Novick, R. P., and Charpentier, E. (2004) *Mol. Microbiol.* **53,** 1515–1527
27. Nizet, V. (2002) *Trends Microbiol.* **10,** 575–580
28. Datta, V., Myskowski, S. M., Kwinn, L. A., Chiem, D. N., Varki, N., Kansal, R. G., Kotb, M., and Nizet, V. (2005) *Mol. Microbiol.* **56,** 681–695
29. González-Mariscal, L., Betanzos, A., Nava, P., and Jaramillo, B. E. (2003) *Prog. Biophys. Mol. Biol.* **81,** 1–44
30. Schneeberger, E. E., and Lynch, R. D. (2004) *Am. J. Physiol. Cell Physiol.* **286,** C1213–C1228
31. Madara, J. L., and Stafford, J. (1989) *J. Clin. Invest.* **83,** 724–727
32. Ma, T. Y., Boivin, M. A., Ye, D., Pedram, A., and Said, H. M. (2005) *Am. J. Physiol. Gastrointest. Liver Physiol.* **288,** G422–G430
33. Al-Sadi, R. M., and Ma, T. Y. (2007) *J. Immunol.* **178,** 4641–4649
34. Chun, J., and Prince, A. (2009) *Cell Host Microbe* **5,** 47–58
35. Rios-Doria, J., Day, K. C., Kuefer, R., Rashid, M. G., Chinnaiyan, A. M., Rubin, M. A., and Day, M. L. (2003) *J. Biol. Chem.* **278,** 1372–1379
36. Nizet, V., Beall, B., Bast, D. J., Datta, V., Kilburn, L., Low, D. E., and De Azavedo, J. C. (2000) *Infect. Immun.* **68,** 4245–4254
37. Carr, A., Sledjeski, D. D., Podbielski, A., Boyle, M. D., and Kreikemeyer, B. (2001) *J. Biol. Chem.* **276,** 41790–41796
38. Dale, J. B., Chiang, E. Y., Hasty, D. L., and Courtney, H. S. (2002) *Infect. Immun.* **70,** 2166–2170
39. Lee, S. W., Mitchell, D. A., Markley, A. L., Hensler, M. E., Gonzalez, D., Wohlrab, A., Dorrestein, P. C., Nizet, V., and Dixon, J. E. (2008) *Proc. Natl. Acad. Sci. U.S.A.* **105,** 5879–5884
40. Ofek, I., Zafriri, D., Goldhar, J., and Eisenstein, B. I. (1990) *Infect. Immun.* **58,** 3737–3742
41. Humar, D., Datta, V., Bast, D. J., Beall, B., De Azavedo, J. C., and Nizet, V. (2002) *Lancet* **359,** 124–129
42. Engleberg, N. C., Heath, A., Vardaman, K., and DiRita, V. J. (2004) *Infect. Immun.* **72,** 623–628
43. Fuller, J. D., Camus, A. C., Duncan, C. L., Nizet, V., Bast, D. J., Thune, R. L., Low, D. E., and De Azavedo, J. C. (2002) *Infect. Immun* **70,** 5730–5739
44. Tsai, P. J., Kuo, C. F., Lin, K. Y., Lin, Y. S., Lei, H. Y., Chen, F. F., Wang, J. R., and Wu, J. J. (1998) *Infect. Immun.* **66,** 1460–1466
45. Cleary, P. P., and Cue, D. (2000) *Subcell. Biochem.* **33,** 137–166
46. Podbielski, A., Beckert, S., Schattke, R., Leithauser, F., Lestin, F., Gossler, B., and Kreikemeyer, B. (2003) *Int. J. Med. Microbiol.* **293,** 179–190
47. Wessels, M. R. (2005) *J. Infect. Dis.* **192,** 13–15
48. McKay, D. M., and Singh, P. K. (1997) *J. Immunol.* **159,** 2382–2390
49. Klenk, M., Koczan, D., Guthke, R., Nakata, M., Thiesen, H. J., Podbielski, A., and Kreikemeyer, B. (2005) *Cell Microbiol.* **7,** 1237–1250
50. Kreikemeyer, B., McIver, K. S., and Podbielski, A. (2003) *Trends Microbiol.* **11,** 224–232
51. Engleberg, N. C., Heath, A., Miller, A., Rivera, C., and DiRita, V. J. (2001) *J. Infect. Dis.* **183,** 1043–1054
52. Sumby, P., Whitney, A. R., Graviss, E. A., DeLeo, F. R., and Musser, J. M. (2006) *PLoS Pathog.* **2,** e5
53. Walker, M. J., Hollands, A., Sanderson-Smith, M. L., Cole, J. N., Kirk, J. K., Henningham, A., McArthur, J. D., Dinkla, K., Aziz, R. K., Kansal, R. G., Simpson, A. J., Buchanan, J. T., Chhatwal, G. S., Kotb, M., and Nizet, V. (2007) *Nat. Med.* **13,** 981–985
54. Levin, J. C., and Wessels, M. R. (1998) *Mol. Microbiol.* **30,** 209–219
55. Bernish, B., and van de Rijn, I. (1999) *J. Biol. Chem.* **274,** 4786–4793
56. Federle, M. J., McIver, K. S., and Scott, J. R. (1999) *J. Bacteriol.* **181,** 3649–3657
57. Graham, M. R., Smoot, L. M., Migliaccio, C. A., Virtaneva, K., Sturdevant, D. E., Porcella, S. F., Federle, M. J., Adams, G. J., Scott, J. R., and Musser, J. M. (2002) *Proc. Natl. Acad. Sci. U.S.A.* **99,** 13855–13860
58. Shao, H., Chou, J., Baty, C. J., Burke, N. A., Watkins, S. C., Stolz, D. B., and Wells, A. (2006) *Mol. Cell Biol.* **26,** 5481–5496
59. Rios-Doria, J., and Day, M. L. (2005) *Prostate* **63,** 259–268